

Spherulitic Structure Development during Crystallization in Confined Space II. Effect of Spherulite Nucleation at Borders

E. Piorkowska,¹ N. Billon,² J. M. Haudin,² K. Gadzinowska¹

¹Centre of Molecular and Macromolecular Studies, Polish Academy of Sciences, 90 363 Lodz, Poland

²Ecole des Mines de Paris, Centre de Mise en Forme des Materiaux, UMR CNRS 7635, BP 207, 06 904 Sophia Antipolis, France

Received 29 December 2004; accepted 10 February 2005

DOI 10.1002/app.21802

Published online in Wiley InterScience (www.interscience.wiley.com).

ABSTRACT: This paper is devoted to the formation of a spherulitic pattern in polymers that are spatially confined. The nucleation at sample boundaries influences the spherulitic structure and accelerates the local conversion of melt into spherulites. A model of the spherulitic pattern formation in narrow strips of polymer based on the probability theory was developed to account for the effect of spherulite nucleation at sample borders. The model allows us to predict the rates of formation of the interspherulitic boundaries and also the distributions of distances from spherulite centers to the boundaries for an isothermal as well as a noniso-

thermal crystallization. The final length of interspherulitic lines and the final number of triple points between spherulites can also be calculated. The predictions of the model were verified by computer simulation, which reproduces spherulitic patterns observed experimentally in strips of thin films. © 2005 Wiley Periodicals, Inc. *J Appl Polym Sci* 97: 2319–2329, 2005

Key words: crystallization; spherulites; microstructure; isotactic polypropylene; spatial confinement

INTRODUCTION

The theory describing a development of the spherulitic structure deals primarily with the conversion of a melt into spherulites. While initial formulations by Avrami and Evans^{1,2} concerned isothermal crystallization in an infinite body, later the theory was developed to describe processes in more complex conditions: nonisothermal conditions [e.g., Refs. 3, 4], volume confinement,^{5–11} and the presence of reinforcing fibers,¹² including the effects of transcrystallinity resulting from intense spherulitic nucleation at sample borders and on fibers.

While the conversion of melt into spherulites is of great interest, a spherulitic pattern is also of importance, since it influences properties of semicrystalline polymeric materials. Interspherulitic boundaries and multiple boundary points, which are weak spots of structure, affect the ultimate mechanical properties and other properties, e.g., gas sorption phenomena [e.g., Refs. 13–15].

In an infinite body, after time t , elapsed from the first nucleation event, the conversion degree is ex-

pressed by the classic formula: $1 - \exp[-E_\infty(t)]$, where the second component equals the probability that arbitrarily chosen sample point remains at time t outside of any spherulite. E is determined by the time dependencies of a nucleation rate, $F(t)$, and a growth rate, $G(t)$, of spherulites [e.g., Refs. 1, 4]:

$$E_\infty(t) = k\pi \int_0^t F(\tau) \left[\int_\tau^t G(s) ds \right]^n d\tau \quad (1)$$

where k and n equal 1 and 2 in a two-dimensional case and 4/3 and 3 in a three-dimensional case, respectively.

When a limited polymer portion in the form of a plate or a strip of film is considered, the probability that a certain point remains unoccluded depends on distances from both polymer borders; the lack of spherulites beyond the material borders slows down the conversion of the melt but an additional spherulitic nucleation at polymer borders accelerates the conversion. To describe the kinetics of the conversion in this case it is necessary to subtract and add the appropriate components to the right side of Eq. (1).^{8–10}

The efforts to describe mathematically the formation of interspherulitic borders were limited initially to crystallization far from the material limits.^{16–19} They were based on considerations of the probability of nucleation event occurrence in space and in time

Correspondence to: Ewa Piorkowska (epiorkow@bilbo.cbmm.lodz.pl).

resulting, in the course of growth, in contacts of respective numbers of crystallizing fronts. Further development of this approach enabled us to account for the effect of material borders in development of the interspherulitic boundaries and of the final spherulitic pattern in narrow strips of polymer films.²⁰ The regions adjacent to the polymer borders differ considerably from the polymer interior; the effect is significant within a distance comparable with the average spherulite size. The decrease of the film width influences the spherulitic structure and leads to a diminished amount of interspherulitic boundaries. The process of formation of triple points and especially of interspherulitic boundary lines is different in narrow strips of films than in films of infinite width. This is because some interspherulitic lines are formed at large distances from spherulite centers at a late stage of crystallization.

In Ref. 20 the spherulitic nucleation at sample edges was not considered. In real systems such nucleation is a frequent phenomenon; very intense nucleation at sample borders leads to transcrystallinity, reflected both in the overall crystallization kinetics and in the spherulitic pattern. Similar effects are frequently observed in fiber-reinforced composites, where intense spherulite nucleation on fiber surfaces is caused by mechanical stress at the interface between a fiber and a supercooled polymer melt and leads to a structure that is indistinguishable from a transcrystalline morphology.²¹

A computer simulation was frequently employed to verify theoretical predictions concerning the spherulitic crystallization and also to visualize emerging spherulitic patterns.^{6,8-10,12,18-20,22,23} The computer modeling was also a valuable tool allowing us to predict overall crystallization kinetics in cases where mathematical description was insufficient, like in the cases of thin films and bulk of fiber-reinforced thermoplastics.²⁴⁻²⁶ The crystallization kinetics and spherulitic morphology are controlled by a number of factors: bulk nucleation density, nucleation density on fiber surfaces, fiber volume fraction, fiber diameter, and spherulitic growth rate. Different effects of fiber presence on crystallization observed experimentally are explained by those dependencies.^{27,28} The computer simulation was also used to determine the nucleation density on fiber surfaces in fiber-reinforced composites based on experimental crystallization data.²⁸ However, the computer simulation of spherulitic crystallization has not been used until now for quantitative description of interspherulitic boundaries in a polymer portion limited by borders that nucleate spherulites.

This paper is devoted to the problem of the influence of spherulite nucleation at sample borders on the formation and final form of the spherulite pattern. The aim of the work was to develop further the probabi-

listic model to enable the analytical description of the formation of interspherulitic boundaries in the presence of spatial borders when spherulite nucleation occurs at those borders. Analytical equations derived in the paper allow the quantification of the effect of the spherulite nucleation on emerging spherulitic patterns, which was not possible thus far. Various sample widths and spherulite nucleation intensities at sample borders are considered.

Computer simulation of spherulitic structures was also conducted as an independent way of obtaining the data describing the interspherulitic boundaries as a function of the polymer film width and to verify predictions of the mathematical model. The computer-simulated samples are visualized and compared with experimentally crystallized spherulite patterns.

So far we have concentrated our efforts on 2D crystallization, that is, on crystallization in thin films. Such geometry allows us to verify the model by comparison with polymer morphologies studied directly by light microscopy and generated by computer simulation.

However, further development of the presented approach will allow us to deal with bulk crystallization as well, including cylindrical morphologies in fiber-reinforced composites. The confined two-dimensional portions of a polymer, as described in this paper, are already representative for two-dimensional fiber-reinforced composites.

PROBABILISTIC MODEL

The application of the probability theory to the characterization of the spherulitic pattern development during the isothermal as well as the nonisothermal crystallization in thin films having infinite and finite width is outlined in Refs. 16-20. During two-dimensional spherulitic crystallization a boundary between two neighboring spherulites has the form of a line, while three spherulites come to contact at a point. The probability of the formation of a contact point among four spherulites on a plane can be neglected.¹⁷ In the case of instantaneous nucleation the probability of a point to be included in a boundary is only constrained by geometric factors. Let us consider an arbitrarily chosen point P in a strip of width $2h$ (Fig. 1) located at distances s_1 and s_2 from the sample borders. The boundary between two spherulites passes through point P on the condition that distances, r , from both spherulite centers to point P are equal with the accuracy of an infinitely small dr . The prerequisite is that spherulites must be nucleated inside a fictitious ring of radius r and width dr . For the spherulites nucleated inside the sample this means that they must be nucleated within the area elements $rdrd\varphi_1$ and $rdrd\varphi_2$.²⁰ The ranges of angles φ_1 and φ_2 depend on the relation between r and distances s_1 and s_2 since the considered ring can be truncated either on one or on both sides by

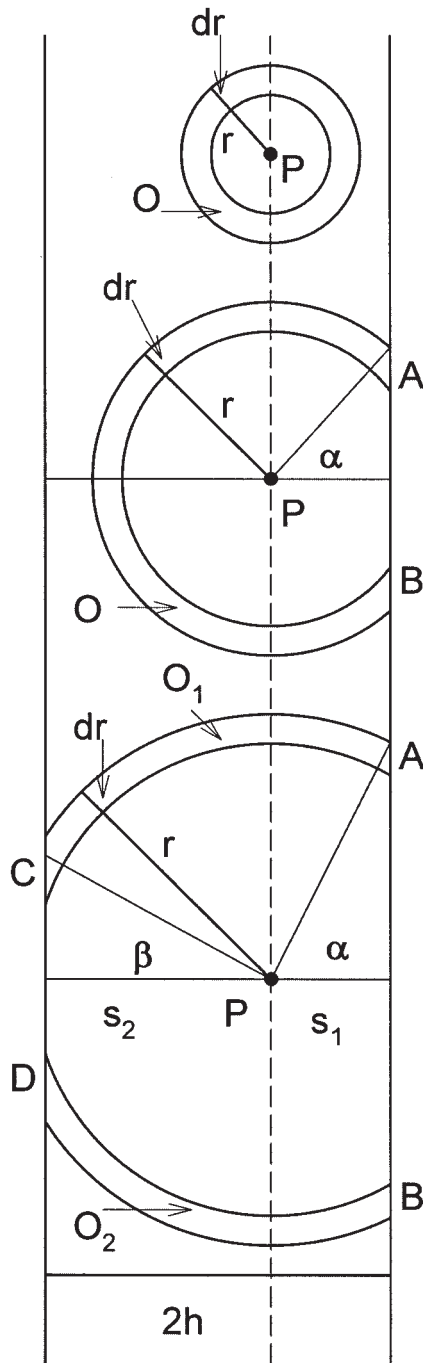


Figure 1 Scheme of fictitious ring of radius r and width dr around point P in a narrow strip of film.

the sample borders, as shown in Figure 1. The parts of the ring confined by the sample borders are denoted in Figure 1 as O for $r < s_2$, O_1 and O_2 for $r > s_2$.

The spherulites nucleated at border participate in the formation of a boundary at the considered point P if the distance from point P to the border is smaller than r . Figure 1 shows schematically three possible situations when the boundary can be formed at point P : (1) by spherulites nucleated inside the sample, (2)

by spherulites nucleated inside the sample and by spherulites nucleated at one edge, and (3) by spherulites nucleated inside the sample and at both borders of the sample. To form a boundary at point P , at distance r from spherulite centers, the spherulites must be nucleated at sections of the borders confined within a ring having a radius r and width dr : these positions are marked in Figure 1 by A , B , C , and D . The length of those sections on the respective borders equals

$$dL_1 = r[r^2 - s_1^2]^{-1/2} dr \quad (2a)$$

$$dL_2 = r[r^2 - s_2^2]^{-1/2} dr \quad (2b)$$

For instantaneous nucleation the probability that n spherulites are nucleated in a certain area dS_1 is expressed by the Poisson formula: $\exp(-E_1) (E_1)^n / n!$, where the expectancy E_1 is the product of dS_1 and the nucleation density. The probability, q_2 , of two spherulites to be nucleated, the first in dS_1 and the second in dS_2 , equals $\exp(-E_1 - E_2) E_1 E_2$, where E_1 and E_2 are the products of dS_1 and dS_2 and the respective nucleation densities. The second condition for the boundary to be formed at point P must be fulfilled: no other than the two considered spherulites can be nucleated inside the circle of radius r around point P , that is, neither inside the sample nor at the sample edges. The probability that no other nucleation event occurs inside the circle, q_0 , equals $\exp[-E + E_1 + E_2]$ with E given by the formula⁹

$$E = D[\pi r^2 - W(r, s_1) - W(r, s_2)] + D_s[Y(r, s_1) + Y(r, s_2)] \quad (3a)$$

$$\text{for } r < s: W(r, s) = 0 \text{ and } Y(r, s) = 0 \quad (3b)$$

for $r > s$:

$$W(r, s) = r^2 \arctan [(r^2/s^2 - 1)^{1/2}] - s(r^2 - s^2)^{1/2} \quad (3b)$$

$$\text{and } Y(r, s) = 2(r^2 - s^2)^{1/2} \quad (3c)$$

Thus, the probability, P_2 , that the boundary line between the respective spherulites passes through point P , equal to a product of q_2 and q_0 , is expressed by the formula

$$P_2(r, s_1, s_2) = \exp[-E(r, s_1, s_2)] E_1 E_2 \quad (4)$$

If a boundary line between spherulites nucleated inside the sample is considered, the product $E_1 E_2$ equals $(D r dr)^2 d\varphi_1 d\varphi_2$. For the boundary formed between a spherulite nucleated inside the sample and a

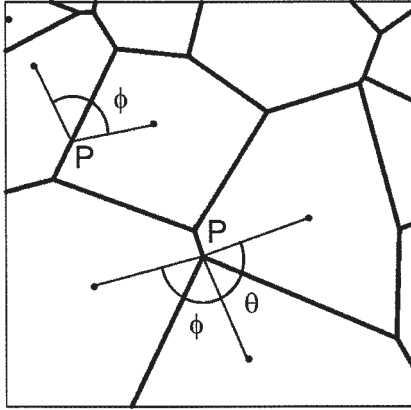


Figure 2 Schematic location of spherulite centers of around the boundary point *P* in a film.

spherulite nucleated at the sample border, the respective expressions are either $Drdrd\varphi_1D_s dL_1$ or $Drdrd\varphi_1D_s dL_2$, where D_s denotes the nucleation density on the sample borders. Finally, for the boundary between spherulites nucleated at the borders the product E_1E_2 equals $(D_s dL_1)^2$, $(D_s dL_2)^2$, or $D_s^2 dL_1 dL_2$. Recalculation of the probability P_2 to the probability that point *P* is included in a boundary element of length dl requires the multiplication of P_2 by the factor $2\sin(\phi/2)/dr$,²⁰ where ϕ is the difference in angular positions of the respective spherulite centers around point *P*, as schematically shown in Figure 2.

A triple point, at intersection of boundary lines, is formed at *P* at a distance r from three spherulite centers on the following condition: these three spherulites must be nucleated inside the ring of radius r and of width dr as shown in Figure 1. In addition, no other spherulite can be nucleated inside the circle of radius r around point *P*. The probability, P_3 , that the triple boundary point is formed at a distance r from three spherulite centers is calculated in a similar way as for the boundary between two spherulites:

$$P_3(r,s_1,s_2) = \exp[-E(r,s_1,s_2)]E_1 E_2 E_3 \quad (5)$$

Similarly as for boundaries between two spherulites, E_i , $i = 1,2,3$, can be expressed in the form of $Drdrd\varphi_1$, $Drdrd\varphi_2$, $D_s dL_1$, and $D_s dL_2$. There is one important difference with respect to the formation of interspherulitic lines: the triple boundary points cannot be formed by spherulites nucleated instantaneously at the same sample border, since boundary lines between those spherulites are parallel and never cross. The recalculation of the probability P_3 to the number of triple points requires multiplication of P_3 by the factor of $4 \sin(\phi/2)\sin(\theta/2)\sin(\gamma/2)/dr^2$,²⁰ where $\gamma = 2\pi - \phi - \theta$, ϕ and θ are differences in angular positions of the respective spherulite centers around point *P*, as shown in Figure 2.

While for certain r , s_1 , and s_2 the positions of spherulites nuclei at the sample edges are fixed, inside the sample the centers of spherulites can be located in two ranges of angle: (1) from α to $\pi - \beta$ and (2) from $\pi + \beta$ to $2\pi - \alpha$ (Fig. 1), where α and β depend on the distances r , s_1 , and s_2 : $\alpha = 0$ for $r < s_1$, and $\alpha = \arctan\{[(r/s_1)^2 - 1]^{1/2}\}$ for $r > s_1$, $\beta = 0$ for $r < s_2$, and $\beta = \arctan\{[(r/s_2)^2 - 1]^{1/2}\}$ for $r > s_2$. The integration over the appropriate ranges of angles allows us to calculate the length of boundary lines and the number of triple points per unit surface area of the sample at distances r from spherulite centers and at distances s_1 and s_2 from the sample borders. All possible combinations of positions of spherulite centers must be considered, and for n centers nucleated inside the strip within the same angle range, the result of integration should be divided by $n!$ to avoid multiple counting of the same events. The final expressions for the boundary length, F_2 , and the number of triple points, F_3 (formed at distance r from centers of contributing spherulites and at distances s_1 and s_2 from the sample borders, both per unit surface area), involve sums of the partial functions representing dif-

TABLE I
Component Functions for the Probabilistic Description of Interspherulitic Lines between Spherulites with Differently Positioned Centers, as indicated in Fig. 1.

Relation among r , s_1 , and s_2	Positions of spherulite centers	Function
$r < s_1$ $s_2 > r > s_1$	O O	$U_1 = 8 \pi D^2 r^2$
	O O	$U_1 = 8 D^2 r^2 [\pi - \alpha - (r^2 - s_1^2)^{1/2} r^{-1}]$
$r > s_2$	AB	$U_2 = 2 D_s^2 r (r^2 - s_1^2)^{-1/2}$
	AO, BO	$U_3 = 8 D D_s r (r^2 - s_1^2)^{-1/2} (r + s_1)$
	(O ₁ + O ₂) (O ₁ + O ₂)	$U_1 = 8 D^2 r \{(\pi - \alpha - \beta)r - (r^2 - s_1^2)^{1/2} - (r^2 - s_2^2)^{1/2} + 2[(r - s_1)(r - s_2)]^{1/2}\}$
	AB, CD	$U_2 = 2 D_s^2 r [(r^2 - s_1^2)^{-1/2} + (r^2 - s_2^2)^{-1/2}]$
	A (O ₁ + O ₂), B (O ₁ + O ₂)	$U_3 = 8 D D_s r (r^2 - s_1^2)^{-1/2} [r + s_1 - [(r - s_2)(r + s_1)]^{1/2}]$
C(O ₁ + O ₂), D(O ₁ + O ₂)	$U_4 = 8 D D_s r (r^2 - s_2^2)^{-1/2} [r + s_2 - [(r + s_2)(r - s_1)]^{1/2}]$	
AC, AD, BD, BC	$U_5 = 4 D_s^2 r [(r - s_1)(r - s_2)]^{-1/2}$	

Note. (O₁ + O₂) denotes that a spherulite center is located either in the O₁ or in the O₂ part of the ring. Function U_1 is from Ref.[20].

TABLE II
Component Functions for the Probabilistic Description of Triple Points between Spherulites with Differently Positioned Centers, as indicated in Fig. 1

Relation among r , s_1 , and s_2	Positions of spherulite centers	Function
$r < s_1$	O O O	$V_1 = 4 \pi^2 D^3 r^3$
$s_2 > r > s_1$	O O O A B O	$V_1 = 4D^3 r [r^2(\pi - \alpha)^2 - 2(r^2 - s_1^2) - s_1(\pi - \alpha)(r^2 - s_1^2)^{1/2}]$ $V_2 = 4 D_s^2 D r [(\pi - \alpha) s_1 (r^2 - s_1^2)^{-1/2} + 1]$
$r > s_2$	A O O, B O O (O ₁ + O ₂)(O ₁ + O ₂)(O ₁ + O ₂)	$V_3 = 4 D_s^2 D^2 r [(\pi - \alpha)(r^2 - s_1^2)^{-1/2}(r^2 + 2s_1^2) + 3s_1]$ $V_1 = 4D^3 r^3 \{(\pi - \alpha - \beta)^2 - 0.5(\pi - \alpha - \beta) [\sin(2\alpha) + \sin(2\beta)] + \cos(2\alpha) + \cos(2\beta) + 2[\cos(\alpha - \beta) - \cos(\alpha + \beta) - 1]\}$
	AB(O ₁ + O ₂)	$V_2 = 4D_s^2 D [(\pi - \alpha - \beta) \cos \alpha + \sin \alpha - \sin \beta] r^2 (r^2 - s_1^2)^{-1/2}$
	CD(O ₁ + O ₂)	$V_3 = 4D_s^2 D [(\pi - \alpha - \beta) \cos \beta - \sin \alpha + \sin \beta] r^2 (r^2 - s_2^2)^{-1/2}$
	AO ₁ O ₁ , BO ₂ O ₂ , CO ₁ O ₁ , DO ₂ O ₂	$V_4 = 4 D_s D^2 r^3 [(\pi - \alpha - \beta) - 1.5 \sin(\alpha + \beta) - 0.5(\pi - \alpha - \beta) \cos(\alpha + \beta)] [(r^2 - s_1^2)^{-1/2} + (r^2 - s_2^2)^{-1/2}]$
	AO ₂ (O ₁ + O ₂), BO ₁ (O ₁ + O ₂)	$V_5 = 2 D_s D^2 r^3 (r^2 - s_1^2)^{-1/2} \{(\pi - \alpha - \beta)[4\cos^2 \alpha + \cos(\alpha + \beta)] + 4\sin(\alpha - \beta) - \sin(2\beta) + 3\sin(2\alpha) - \sin(\alpha + \beta)\}$
	CO ₂ (O ₁ + O ₂), DO ₁ (O ₁ + O ₂)	$V_6 = 2 D_s D^2 r^3 (r^2 - s_2^2)^{-1/2} \{(\pi - \alpha - \beta)[4\cos^2 \beta + \cos(\alpha + \beta)] + 4 \sin(\beta - \alpha) + 3\sin(2\beta) - \sin(2\alpha) - \sin(\alpha + \beta)\}$
	AC(O ₁ + O ₂), BD(O ₁ + O ₂)	$V_7 = 4D_s^2 D r^3 [(r^2 - s_2^2)(r^2 - s_1^2)]^{-1/2} \cos[(\alpha + \beta)/2] \{2\cos[(\alpha + \beta)/2] - \cos[(\alpha - \beta)/2] (\cos \alpha + \cos \beta) + \sin [(\beta - \alpha)/2] (\sin \alpha - \sin \beta)\}$
	AD(O ₁ + O ₂), BC(O ₁ + O ₂)	$V_8 = 4D_s^2 D r^3 [(r^2 - s_2^2)(r^2 - s_1^2)]^{-1/2} \cos[(\beta - \alpha)/2] \{ \cos[(3\beta + \alpha)/2] + \cos[(\beta + 3\alpha)/2] + 2\cos [(\beta - \alpha)/2] \}$
	ABC, ABD, ACD, CBD	$V_9 = 16D_s^3 r^2 [(r^2 - s_2^2)(r^2 - s_1^2)]^{-1/2} \cos[(\alpha + \beta)/2] \cos [(\alpha - \beta)/2]$

Note. (O₁ + O₂) denotes that a spherulite center is located either in the O₁ or in the O₂ part of the ring. Function V₁ is from Ref. [20].

ferent combinations of spherulite positions, listed in Tables I and II.

$$\text{For } r < s_1: F_2 dr = U_1 \exp(-E) dr \quad (6a)$$

$$F_3 dr = V_1 \exp(-E) dr \quad (6b)$$

For $s_2 > r > s_1$:

$$F_2 dr = (U_1 + U_2 + U_3) \exp(-E) dr \quad (6c)$$

$$F_3 dr = (V_1 + V_2 + V_3) \exp(-E) dr \quad (6d)$$

For $r > s_2$:

$$F_2 dr = (U_1 + \dots + U_5) \exp(-E) dr \quad (6e)$$

$$F_3 dr = (V_1 + \dots + V_9) \exp(-E) dr \quad (6f)$$

The appropriate selection of the functions V_i and U_i enables us to differentiate boundaries formed between spherulites nucleated inside the sample, between spherulites nucleated at borders, and between these two populations of spherulites.

The distribution of distances from spherulites centers to the boundary lines between these spherulites, $R_2(r, s_1, s_2)$, and the distribution of distances from the

spherulite centers to the triple boundary points formed by these spherulites, $R_3(r, s_1, s_2)$, are obtained by multiplication of the functions F_2 and F_3 by the number of the spherulites participating in the formation of the respective structure element:

$$R_2(r, s_1, s_2) dr = 2F_2(r, s_1, s_2) dr$$

$$\text{and } R_3(r, s_1, s_2) dr = 3F_3(r, s_1, s_2) dr \quad (7)$$

In the case of instantaneous nucleation the distance from spherulite center to the boundary of this spherulite, r , always equals $\int_0^t G(u) du$, where t denotes the time of boundary formation and $G(u)$ is the time-dependent growth rate. Hence, substituting this integral for r and $G(t) dt$ for dr in Eqs.(6a) and (6b) one obtains the rate of interspherulitic lines formation $H_2(t, s_1, s_2)$, and the rate of triple points formation, $H_3(t, s_1, s_2)$, in unit area of the film at distances s_1 and s_2 from the sample boundaries. For the isothermal crystallization with $G = \text{const.}$ they are

$$H_2(t, s_1, s_2) dt = F_2(Gt, s_1, s_2) G dt$$

$$\text{and } H_3(t, s_1, s_2) dt = F_3(Gt, s_1, s_2) G dt \quad (8)$$

To obtain the average rates of boundary formation and the distance distributions from centers to bound-

aries in the entire strip, one must perform integration over the range $0 < s_1 < h$ and divide the result by h :

$$H_{av}(t, 2h) = h^{-1} \int_0^h H(t, s_1, 2h - s_1) ds_1$$

$$\text{and } R_{av}(r, 2h) = h^{-1} \int_0^h R(r, s_1, 2h - s_1) ds_1 \quad (9)$$

The boundary length, L_2 , and the number of boundary points, L_3 , formed until time t are obtained by the respective integration,

$$L_n(t, 2h) = h^{-1} \int_0^t \int_0^h H_n(t', s_1, 2h - s_1) ds_1 dt'$$

for $n = 2$ and $n = 3$ (10)

The length of interspherulitic lines and the number of triple boundary points per unit area of a sample after a completion of crystallization are equal to $L_2(\infty, 2h)$ and $L_3(\infty, 2h)$, respectively.

To demonstrate the influence of the nucleation at borders of thin film on the development of the spherulitic pattern, the rates and the progression of boundaries formation and distribution of length and number of interspherulitic boundaries across the sample were calculated for samples of various width, according to formulas derived in this section. The following data were used: $G = 5$ unit/min and $D = 6.25 \times 10^{-4}$ unit⁻², which corresponds to an average spherulite radius in infinite sample about 22 units. To represent a weak and intense nucleation at borders two values of nucleation density were selected: $D_s = 0.025$ unit⁻¹ and $D_s = 0.5$ unit⁻¹. Also, calculations for cases where nucleation inside the sample was absent ($D = 0$) were conducted to test the elaborated approach.

The conversion degree for both infinite and finite samples were also calculated taking advantage of the formulae derived in Refs. 8, 9, 16–19.

COMPUTER SIMULATION

Computer simulation is a way to verify such an approach, provided that it accounts for the same basic assumptions.

The 2D version of previously developed software^{22,23} was used to reproduce polymer spherulitic crystallization, that is, nucleation and growth of circular entities. The sample was assumed to be a rectangle of finite width, $2h$, and length, L . The instantaneous nucleation is represented by nuclei whose density is D per area unit and D_s per unit of border line length. The location of nuclei is chosen at random, using the random number generator of the computer. Growth be-

gins immediately after nucleation and the constant growth rate is equal for all entities. Two coordinates and time of appearance of any possible triple points are simply deduced from the locations and the times of nucleation of spherulites. From all possible triple points real ones are those that appear in a still liquid zone, i.e., outside of all other spherulites. Then, boundaries are calculated accounting for the following considerations.

1. Two spherulites must be close enough to develop a boundary and the first possible boundary point is located on the same straight line as the two spherulite centers. If the point is located in a sample fraction already occupied by another spherulite, then the first point of the boundary to be considered is the closest triple point involving both considered spherulites.

2. The boundary line can develop in two directions apart from the first contact point; hence, the coordinates of successive points are calculated discretising time from the moment of appearance of the first contact point to the current time or to the moment when the considered boundary reaches the closest triple point involving both considered spherulites or the boundary of the sample or a liquid zone (defining here the "last boundary point").

3. In the case of incomplete crystallization, circular boundary solid-liquid exists between given last boundary points unless these boundaries intercept the specimen borders.

Applying the above-described procedure, it is possible to calculate at the same time the location of triple points and points along boundary lines. The surface of all entities, the number of triple points, and the length of all boundary lines are then calculated. The acquired data are plotted, which enables visualization of the emerging spherulitic patterns.

In computer simulation the crystallization kinetics of fictitious sample varies from one calculation to another. As defined during preliminary works, at least 500 runs of simulations for each set of parameters are performed to obtain average results. Additionally, to make our result as representative as possible the fictitious sample is sufficiently long to contain at least 100 spherulites.

EXPERIMENTAL

Ten-micrometer-thick films of isotactic polypropylene (iPP), Malen F401 (having MFI of 3.0 g/10 min (230°C, 2.16 kg), $M_w = 3.0 \times 10^5$ g/mol, $M_w/M_n = 5.3$, manufactured by Orlen SA, Poland) were prepared by compression molding at 190°C and quenched to room temperature. To produce the spherulitic structure in strips of film with intense nucleation at borders, a water suspension of nucleating agent was deposited on iPP film surfaces, leaving only a strip of a finite width uncovered; this procedure was performed un-

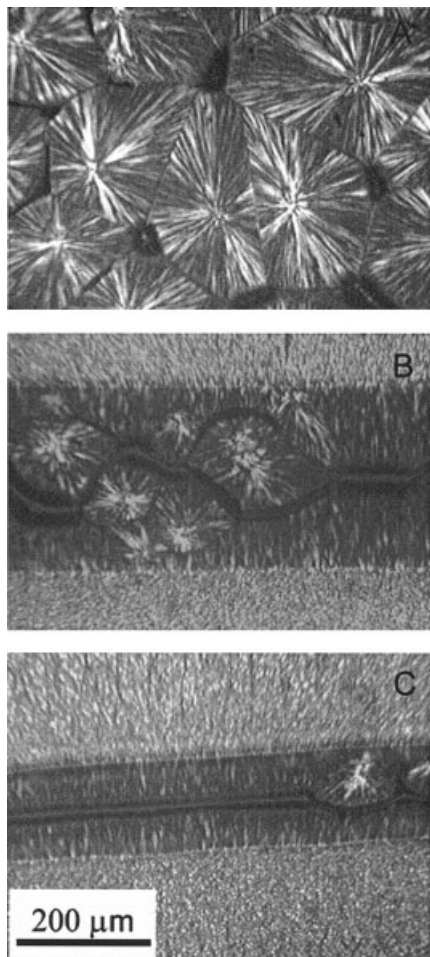


Figure 3 Microphotographs of fragments of iPP films: A, wide film; B, 290- μm -wide strip of film; C, 150- μm -wide strip of film. Strips in B and C are nucleated at sample borders by a strong nucleating agent.

der a magnifying lens. After being dried, the films, with free upper surface, were heated to 220°C, cooled to crystallization temperature of 133°C, and isothermally crystallized in Linkam Hot Stage mounted on a polarized light microscope. The entire procedure was carried out under a flow of pure dry nitrogen. Films without nucleating agent were also crystallized in the same way for comparison.

RESULTS

Figure 3 shows light micrographs of a fragment of a wide iPP film and narrow strips of iPP film, having width of 290 and 150 μm between the areas covered with nucleating agent. Straight interspherulitic boundaries in a wide film indicate that most spherulites were nucleated at the same time. At the edges of narrow strips a very intense spherulite nucleation caused the crystallization in the form of transcrystalline layers. The width of the narrower (150 μm) strip is

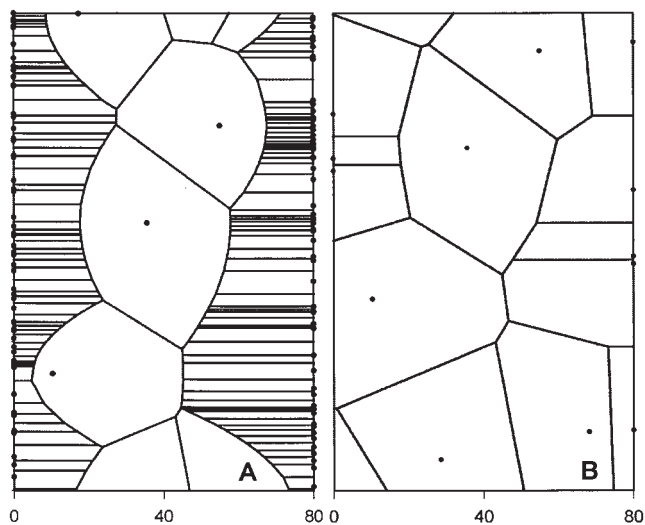


Figure 4 Fragments of computer-simulated thin polymer films having the width of 80 units with the intense spherulite nucleation at sample borders of density 0.5 unit^{-1} (A) and with the weak spherulite nucleation at borders of density 0.025 unit^{-1} (B).

less than the diameter of an average spherulite in the wide sample, which is about 220 μm . The wider strip contains a significant amount of spherulites nucleated inside the polymer, as shown in Figure 3, while the narrower strip is nearly filled with transcrystalline layers nucleated at the edges. The spherulites nucleated inside the strip are seldom visible. The change of

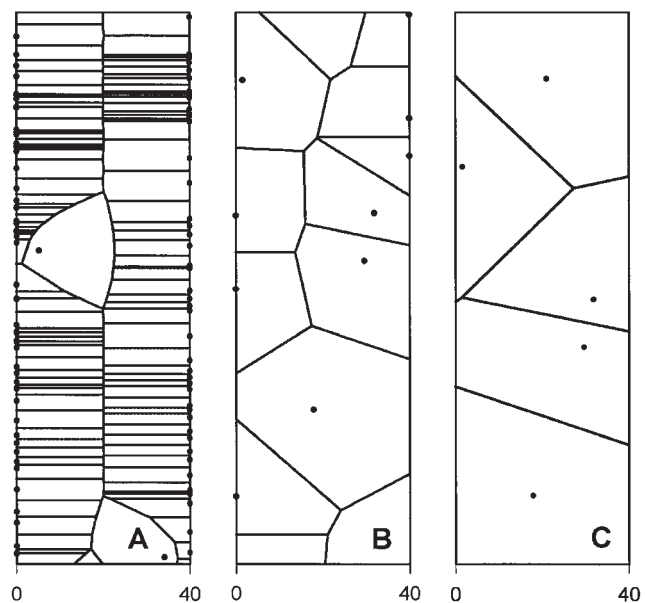


Figure 5 Fragments of computer-simulated thin polymer films having the width of 40 units with the intense spherulite nucleation at sample borders of density 0.5 unit^{-1} (A), with the weak spherulite nucleation at borders having density 0.025 unit^{-1} (B) and with no spherulite nucleation at the borders (C).

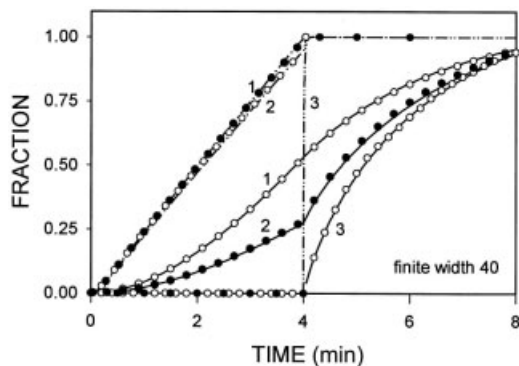


Figure 6 Conversion degree (1) and the progression of boundary lines (2) and triple points (3) formation against time in finite sample 40 units wide with intense (dot-dash lines) and weak (continuous lines) spherulite nucleation at borders, without spherulite nucleation inside the sample. Lines are based on the probabilistic description while symbols denote the results of computer simulation.

volume due to crystallization caused the thinning of films around triple points. In the narrower as well as in the wider strip the thinning of the film and weakening of the boundaries between spherulites nucleated on opposite edges of the strip resulted in fracture of the polymer along the spherulite boundaries.

In Figures 4 and 5 the computer-simulated spherulitic patterns are shown in strips of different width and different nucleation density at borders. The width of the sample shown in Figure 5(a), with intense nucleation at borders, is close to the average spherulite diameter in an infinite sample, while the width of the sample shown in Figure 4 is twice as large. The computer-simulated spherulitic patterns visible in Figures 4a and 5a, with strong nucleation at sample borders, correspond qualitatively to those visible in Figure 3(b) and (c).

Thus, we conclude that the computer simulation allows us to reproduce the spherulitic patterns in narrow strips in a correct way and it is further used to verify the probabilistic description of the crystallization in narrow strips with additional nucleation at the edges of the sample.

Based on Eqs. (6–10) it is expected that the sample width and spherulite nucleation density inside a polymer and at sample borders control the spherulitic crystallization. Thus, all three factors were varied to estimate their effect on the formation of spherulitic pattern and its final form.

First we compared the predictions of the probabilistic description with the results of computer simulation for 40 arbitrary unit wide samples involving the spherulite nucleation only at the borders. This allowed us to exclude from the considerations all functions in Tables I and II containing the nucleation density inside a polymer, D .

Figure 6 shows the progression of the formation of

triple points, interspherulitic boundary lines, and also the conversion degree of melt into spherulites in those samples. A very good agreement between results obtained by computer simulation and based on the probabilistic description was achieved. For the sample with very dense nucleation on edges, with density of 0.5 per unit, the conversion degree is nearly a linear function of time, because the transcrySTALLINE fronts, similar to those visible in Figure 3(c) and 3(d), grow from the sample edges until impingement, abruptly ending the crystallization. The straight line boundaries between those densely nucleated spherulites also progress linearly with time. They are very numerous; thus, the boundary between two fronts formed at the end of crystallization is only a minor fraction of the total boundary length. All triple points are formed suddenly when the two transcrySTALLINE fronts impinge.

The transcrySTALLINE joint front is formed before it is truncated by other spherulites. Thus, sufficient decrease of sample width hinders a development of transcrySTALLINE morphology even in the absence of spherulite nucleation inside the sample. The decrease of nucleation density to 0.025 per unit increases the distance between the nuclei at edges which, on average, equals the sample width. The conversion of melt into spherulites and the formation of the boundaries, depicted in Figure 6, are slower. The progression of the formation of interspherulitic lines changes rapidly when spherulites nucleated at opposite borders come in contact, but still proceeds because the crystallization does not end. All triple points are formed after this moment, but not so rapidly as in the case of dense nucleation.

Further, spherulite nucleation inside a polymer is accounted for. While the constant nucleation density inside a polymer is assumed, the sample width and nucleation density at sample borders are varied to estimate their influence on spherulitic crystallization and morphology.

Figure 7 shows the progression of the formation of triple points and interspherulitic lines and also the conversion degree of melt into spherulites in samples having width of 40 and 20 units, with spherulite nucleation inside, having density of $D = 6.25 \times 10^{-4}$ unit $^{-2}$. Fragments of computer simulated samples, 40 units wide, are shown in Figure 5 together with the fragment of the simulated sample without any nucleation at edges, plotted for comparison.

Figure 8 shows the time dependence of conversion degree and the progression of formation of boundaries in 80 unit wide samples, with weak and dense nucleation on borders, shown in Figure 4, and also in infinite film. Again, very good agreement was reached between the results based on the probabilistic description and obtained by means of computer simulation.

The conversion degree and the progression of the formation of boundaries in a 40 unit wide sample with

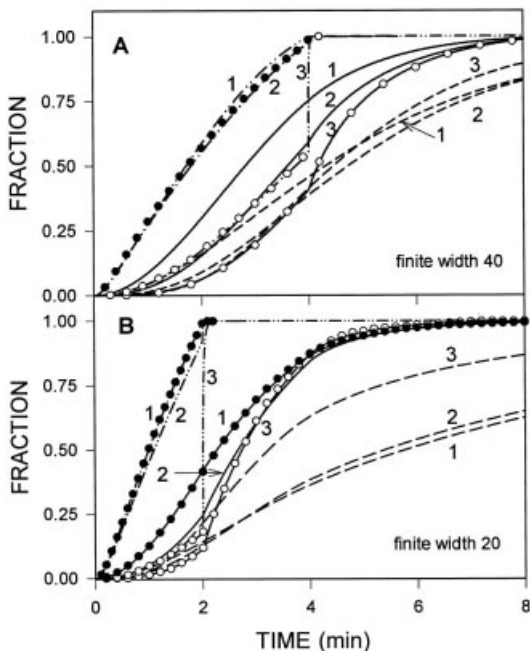


Figure 7 Conversion degree (1) and the progression of boundary lines (2) and triple points (3) formation against time in finite samples with spherulite nucleation inside, having width of 40 units (A) and 20 units (B), with intense spherulite nucleation (dot-dash lines), with weak spherulite nucleation (continuous lines), and without nucleation on borders (dashed lines); the latter is from Ref. 20 Lines are based on the probabilistic description while symbols denote results of computer simulation.

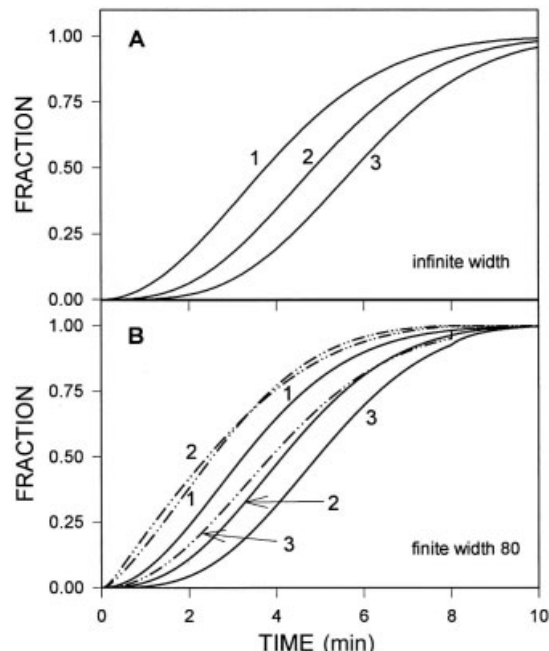


Figure 8 Conversion degree (1), the progression of boundary lines (2), and triple points (3) formation against time in samples with spherulite nucleation inside: (A) infinite width, data from Ref. 20 and (B) width of 80 units, with intense spherulite nucleation (dot-dash lines) and with weak spherulite nucleation (continuous lines) at sample borders.

spherulite nucleation inside does not differ much from those for the sample without such nucleation if the nucleation at the borders is intense. However, about half of the triple points are formed before the transcrystalline fronts meet in the central part of the strip, due to impingement of those fronts with spherulites nucleated inside the strip. When nucleation at the borders is weak the spherulites nucleated inside the strip play a more significant role, accelerating both the conversion of melt into spherulites and the formation of interspherulitic boundaries. The decrease of the sample width to 20 units, which is about the average spherulite radius in an infinite sample, reduces the role of spherulites nucleated inside the strip; hence, the respective dependencies become more similar to those shown in Figure 6, except that all phenomena related to the impingement of spherulites nucleated on opposite borders occur earlier. The nucleation at borders accelerates both the conversion of melt into spherulites and the formation of boundaries compared with that in narrow strips without such nucleation and also in an infinite film with the same nucleation intensity inside the polymer. In the 80 unit wide sample with nucleation at borders the conversion of melt into spherulites and the formation of boundaries are still faster than in an infinite film but the acceleration is not so pro-

nounced as in the case of narrower samples. The difference in the formation of structure caused by the change in the nucleation density at borders is also reduced.

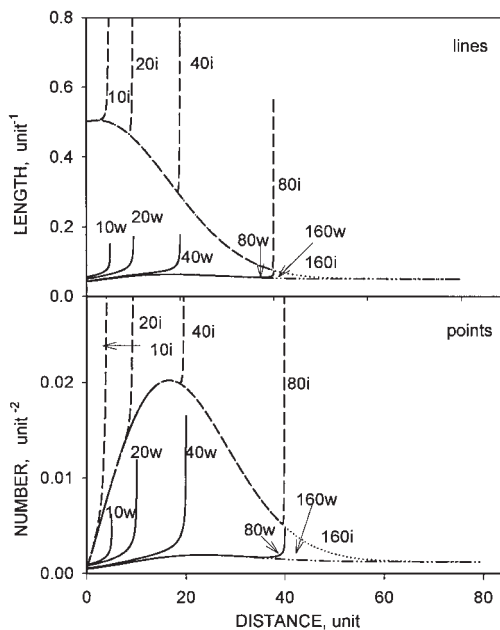


Figure 9 Distributions of length of interspherulitic boundary lines and number of triple points in unit area of film against the distance from the sample border. Numbers denote the width of finite samples expressed in arbitrary units. Symbols w and i denote weak and intense nucleation at sample borders.

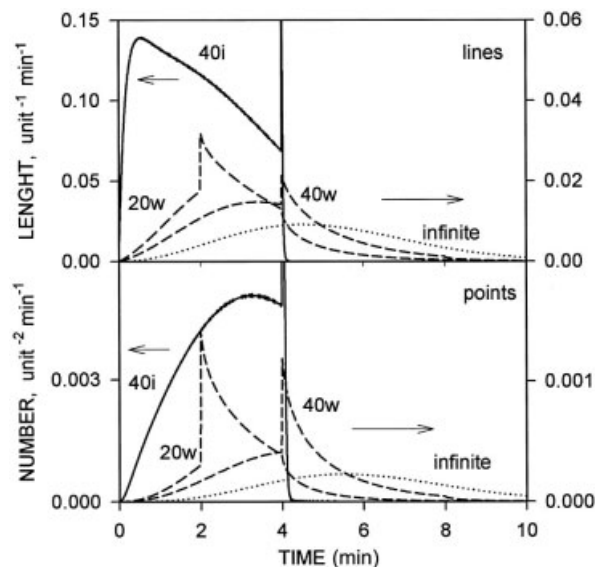


Figure 10 Rates of formation of boundary lines and triple points between spherulites in finite and infinite samples (dotted lines). Numbers denote the width of finite samples expressed in arbitrary units. Symbols *w* and *i* denote weak and intense nucleation at sample borders.

Not only does the progression of the formation of interspherulitic boundaries change due to spherulite nucleation at borders, but also the final length of boundary lines and number of triple points, which is clearly seen in Figures 4 and 5. The profiles of final length of lines and number of triple points per unit area are plotted in Figure 9 for samples of various width with intense and weak nucleation at the borders. In films without such nucleation the areas adjacent to the borders contain fewer interspherulitic boundaries than the sample interior.²⁰ The nucleation at the borders increases the local length of lines and the number of triple points. In sufficiently wide strips of film the number of boundaries in a distance from a border of about 2–3 average spherulite radii achieves the level typical for an infinite film. In narrower strips it increases rapidly in the central zones, due to increased probability of impingement of spherulites nucleated on opposing borders. The effect is enhanced by intense nucleation at sample borders. As this increase is very local, the fraction of such boundaries may not contribute significantly to the average amount of boundaries per unit area. This contribution depends on the relation between the sample width and the nucleation density at the borders, that is, on the average distance between the centers of spherulites nucleated there. In the case of a weak nucleation at the borders the abrupt increase in length of the lines and the number of triple points per unit area in the middle of the sample has a maximum for a certain sample width, as shown in Figure 9.

A final spherulitic pattern can be described quantitatively by distributions of distances from spherulite centers to interspherulitic boundaries. In Figure 10 the rates of the formation of interspherulitic boundaries in 40 and 20 unit wide strips of films are plotted, together with respective curves for infinite films. The recalculation of the dependencies shown in Figure 10 according to Eq. (7) allows us to obtain easily the distributions of distances from spherulite centers to boundaries formed by these spherulites. Spherulite nucleation at the borders of narrow strips causes the fast formation of numerous boundaries between spherulites. This is reflected in the distance distributions from spherulite centers to the boundaries, which differ from those for an infinite film. In narrow strips of films having width equal or less than the average spherulite diameter in an infinite film the distributions exhibit pronounced peaks for distances equal to half of the strip width, which is caused by impingement of spherulites nucleated at opposite borders of the samples.

DISCUSSION AND CONCLUSIONS

In this paper the changes of isothermally crystallized two-dimensional spherulitic structure due to the presence of spherulite nucleation at sample borders were evaluated by means of computer simulation and probabilistic description. The results obtained indicate clearly that even a relatively weak nucleation on borders influences the spherulitic structure. The regions adjacent to the polymer borders, within a distance comparable to the average spherulite diameter, differ considerably from the polymer interior. The process of the formation of triple points and of interspherulitic boundary lines is faster due to the spherulite nucleation at borders. There is no direct relation between the kinetics of the formation and the final form of the spherulitic structure in narrow strips of polymer and in wide films.

Although the results obtained on the basis of the probabilistic description and computer simulation described in this paper concern instantaneous nucleation, the model can be also applied to nucleation prolonged in time. The general formulas are valid for the isothermal as well the nonisothermal processes. It is also possible to distinguish between the interspherulitic boundaries formed either within or between the populations of spherulites nucleated inside the polymer and at material borders. In the case of nucleation at borders so dense that the boundaries within transcrystalline layers are no longer distinguishable, such boundaries can be easily excluded from the considerations.

Here only two-dimensional spherulitic crystallization was studied; however, one can expect similar tendencies in changes of spherulitic structure forma-

tion and in its final form due to spatial limits of a polymer in three dimensions as well. Although the description of the formation of boundaries in three-dimensional polymer portions with one finite dimension is not possible so far, nevertheless both the probabilistic description and the computer simulation methods described here have a potential ability to deal with this problem. Since the probabilistic approach can deal with any localization of nucleation sites, there is a possibility of extending the presented treatment to fiber-reinforced composites, where spherulite nucleation on fibers is frequent. The two-dimensional spherulitic patterns described analytically and computer simulated in this paper are similar to those emerging in thin films of fiber-reinforced composites, either observed experimentally²¹ or computer simulated.²⁴

For the two-dimensional case numerous partial functions describing the boundaries between spherulites nucleated at various localizations resulted from the number of possible localizations for centers of spherulites forming the boundary. In bulk, a spherical cap around the boundary point, which must be considered instead of the ring, will not split into two separate fragments by truncation at the sample borders as it does the ring. At each sample border only one circle instead of two sections will be considered. This greatly simplifies the future application of the elaborated approach to bulk crystallization.

Thin polymer films, being in fact confined portions of a material, are frequently used to study the spherulitic structure of a polymer. Those confined portions can differ significantly from a bulk material. While the intense spherulitic nucleation at sample borders is easily recognizable by microscopic methods and can be taken into account, the weak nucleation, resulting in less obvious changes, also affects the kinetics of the structure formation and the spherulitic pattern.

This work was supported by Coordination Action PIAM, 6-th EFP and by CMMS PAS, project 5.1, 2004.

References

1. Avrami, M. *J Chem Phys* 1939, 7,1103; 1940,8,212; 1941, 9, 177.
2. Evans, U. R. *Trans Faraday Soc* 1945, 41, 365.
3. Ozawa, T. *Polymer* 1971, 12, 150.
4. Nakamura, K.; Katayama, K.; Amano, T. *J Appl Polym Sci* 1973, 17, 1031.
5. Esclaine, J. M.; Monasse, B.; Wey, E.; Haudin, J. M. *Colloid Polym Sci* 1984, 262, 366.
6. Billon, N.; Esclaine, J. M.; Haudin, J. M. *Colloid Polym Sci* 1989, 267, 668.
7. Billon, N.; Haudin, J. M. *Colloid Polym Sci* 1989, 267, 1064.
8. Piorkowska, E. *Colloid Polym Sci* 1997, 275, 1035.
9. Piorkowska, E. *Colloid Polym Sci* 1997, 275, 1046.
10. Billon, N.; Magnet, C.; Lefebvre, D.; Haudin, J. M. *Colloid Polym Sci* 1994, 272, 633.
11. Schultz, J. M. *Macromolecules* 1996, 29, 3022.
12. Piorkowska, E. *Macromol Symp* 2001, 169, 143.
13. Schultz, J. M. *Polym Eng Sci* 1984, 24, 770.
14. Mucha, M.; Kryszewski, M. *Colloid Polym Sci* 1980, 258, 743.
15. Galeski, A.; Koenczoel, L.; Piorkowska, E.; Baer, E. *Nature* 1987, 325, 40.
16. Piorkowska, E.; Galeski, A. *J Polym Sci Polym Phys Ed* 1985, 23, 1723.
17. Piorkowska, E. *J Chem Phys* 1995, 99, 14007.
18. Piorkowska, E. *J Chem Phys* 1995, 99, 14016.
19. Piorkowska, E. *J Chem Phys* 1995, 99, 14024.
20. Piorkowska, E.; Billon, N.; Haudin, J. M.; Kolasinska, J. *J Appl Polym Sci* 2002, 86, 1373.
21. Thomason, J. L.; Van Rooyen, A. A. *J Mater Sci* 1992, 27, 889.
22. Billon, N.; Haudin, J. M. *Ann Chim Fr* 1990, 15, 1.
23. Billon, N.; Monasse, B.; Haudin, J. M.; Chenot, J. L. In *Computer Aided Training in Science and Technology*, Onate, E.; Suarez, B.; Owen, D. R. J.; Shrefler, B.; Kroplin, M.; Kleiher, M.; Eds.; CIMNE, Pineridge Press: Barcelona, 1990 p 384.
24. Mehl, A. N.; Rebenfeld, L. *J Polym Sci B Polym Phys* 1993, 31, 1677.
25. Mehl, A. N.; Rebenfeld, L. *J Polym Sci B Polym Phys* 1993, 31, 1687.
26. Krause, T.; Kalinka, G.; Auer, C.; Hinrichsen, G. *J Appl Polym Sci* 1994, 51, 399.
27. Dean, D. M.; Mehl, N. A.; Rebenfeld, L.; Register, R. A. *J Mater Process Manufact Sci* 1996, 4, 233.
28. Mehl, A. N.; Rebenfeld, L. *J Appl Polym Sci* 1995, 57, 187.